Biochemical and structural studies on the high affinity of Hsp70 for ADP

Akihiko Arakawa,[1,2,3] Noriko Handa,[3] Mikako Shirouzu,[3] and Shigeyuki Yokoyama[1,2,3]*

[1]Department of Biophysics and Biochemistry, Graduate School of Science, The University of Tokyo, Tokyo 113-0033, Japan
[2]Laboratory of Structural Biology, Graduate School of Science, The University of Tokyo, Tokyo 113-0033, Japan
[3]RIKEN Systems and Structural Biology Center, Yokohama City, Kanagawa 230-0045, Japan

Received 14 January 2011; Revised 9 May 2011; Accepted 11 May 2011
DOI: 10.1002/pro.663
Published online 23 May 2011 proteinscience.org

Abstract: The molecular chaperone 70-kDa heat shock protein (Hsp70) is driven by ATP hydrolysis and ADP–ATP exchange. ADP dissociation from Hsp70 is reportedly slow in the presence of inorganic phosphate (P_i). In this study, we investigated the interaction of Hsp70 and its nucleotide-binding domain (NBD) with ADP in detail, by isothermal titration calorimetry measurements and found that Mg^{2+} ion dramatically elevates the affinity of Hsp70 for ADP. On the other hand, P_i increased the affinity in the presence of Mg^{2+} ion, but not in its absence. Thus, P_i enhances the effect of the Mg^{2+} ion on the ADP binding. Next, we determined the crystal structures of the ADP-bound NBD with and without Mg^{2+} ion. As compared with the Mg^{2+} ion-free structure, the ADP- and Mg^{2+} ion-bound NBD contains one Mg^{2+} ion, which is coordinated with the β-phosphate group of ADP and associates with Asp10, Glu175, and Asp199, through four water molecules. The Mg^{2+} ion is also coordinated with one P_i molecule, which interacts with Lys71, Glu175, and Thr204. In fact, the mutations of Asp10 and Asp199 reduced the affinity of the NBD for ADP, in both the presence and the absence of P_i. Therefore, the Mg^{2+} ion-mediated network, including the P_i and water molecules, increases the affinity of Hsp70 for ADP, and thus the dissociation of ADP is slow. In ADP–ATP exchange, the slow ADP dissociation might be rate-limiting. However, the nucleotide-exchange factors actually enhance ADP release by disrupting the Mg^{2+} ion-mediated network.

Keywords: Hsp70; ADP; Mg^{2+} ion; inorganic phosphate; ITC; X-ray crystallography

Introduction

The 70-kDa heat shock protein (Hsp70) family members are conserved in almost all organisms and are involved in many cellular processes, including the correct folding of nascent and/or denatured proteins to prevent their aggregation and the post-translational transport of proteins.[1–4] Hsp70 has an ATP-dependent chaperone activity and contains the N-terminal nucleotide-binding domain (NBD) and the C-terminal substrate-binding domain (SBD). The NBD consists of four subdomains, IA, IB, IIA, and IIB, which surround the ATP/ADP-binding pocket. The SBD is composed of the N-terminal β-sheet subdomain (SBDβ), which binds the substrate polypeptide, and the C-terminal α-helical subdomain, which provides the lid of the SBDβ. Small-angle X-ray scattering experiments[5,6] and real-time Förster

Abbreviations: ADP, adenosine diphosphate; AMPPNP, adenylyl imidodiphosphate; ATP, adenosine triphosphate; BAG, bcl-2 associated athanogene; DTT, dithiothreitol; EDTA, ethylenediaminetetraacetic acid; HEPES, 4-(2-hydroxyethyl)-1-piperazineethanesulfonic acid; HPLC, high performance liquid chromatography; Hsp70, 70-kDa heat shock protein; ITC, isothermal titration calorimetry; NBD, nucleotide-binding domain; P_i, inorganic phosphate; RMSD, root mean square deviation; SBD, substrate-binding domain; TEV, tobacco etch virus.

Grant sponsors: the RIKEN Structural Genomics/Proteomics Initiative (RSGI); the National Project on Protein Structural and Functional Analysis; the Targeted Proteins Research Program from the Ministry of Education, Culture, Sports, Science, and Technology of Japan and Research Fellowship of the Japan Society for the Promotion of Science (to A.A.).

Correspondence to: Shigeyuki Yokoyama, Department of Biophysics and Biochemistry, Graduate School of Science, The University of Tokyo, 7-3-1 Hongo, Bunkyo-ku, Tokyo 113-0033, Japan. E-mail: yokoyama@biochem.s.u-tokyo.ac.jp

resonance energy transfer measurements[7] revealed that the overall conformation of Hsp70 changes upon ATP binding. This conformational change is likely to open the α-helical lid of the SBD, as observed in the ATP-bound Sse1 structure.[8] In this state, the substrate-binding pocket in the SBD is uncovered, and the affinity of Hsp70 for its substrate proteins is consequently low. Next, a J domain cochaperone, such as DnaJ and Hsp40, binds to the NBD to activate ATP hydrolysis by Hsp70 through its J domain, and also recruits its substrate proteins to Hsp70.[9,10] Upon ATP hydrolysis, the Hsp70 conformation changes from the ATP-bound state to the ADP-bound state, in which the substrate-binding pocket is covered by the α-helical lid, and the substrate protein is thereby held tightly.[11,12] Subsequently, Hsp70 releases the ADP and catches a fresh ATP, and as a consequence, Hsp70 returns to the ATP-bound state and releases the refolded protein. In this manner, Hsp70 functions as a molecular chaperone through the ATP cycle.

In the ADP–ATP exchange reaction, Hsp70 releases ADP by itself, through the association of the SBD with the NBD.[13] However, the dissociation rate of ADP is very slow, and the ADP-bound Hsp70 accumulates.[14] In this step, the nucleotide-exchange factors, such as GrpE from prokaryotes and the BAG-family proteins, Hsp110, and HspBP1/Fes1/Sls1 from eukaryotes, interact with the Hsp70 NBD and play important roles. In the crystal structures of the complexes of the NBD and the nucleotide-exchange factors, the interactions of the nucleotide-exchange factors modulate the arrangement of the four subdomains and thereby, disrupt the nucleotide-binding pocket of the NBD, which facilitates the ADP release. As a result, the nucleotide-exchange factors enhance the ADP–ATP exchange reaction of Hsp70.[15–21] Actually, the presence of the nucleotide-exchange factors improves the chaperone activity of Hsp70.[17–20] Such nucleotide-exchange factors in the ATP cycle are needed, because of the slow dissociation rate of ADP from Hsp70. Furthermore, inorganic phosphate (P_i) lowers the ADP dissociation rate by several folds.[22–26]

In this study, the interaction of Hsp70 with ADP was analyzed biochemically and structurally. First, we performed isothermal titration calorimetry (ITC) measurements to investigate the affinities of Hsp70 and its NBD for ADP in detail, and found that ADP binds tightly to Hsp70 in a Mg^{2+} ion-dependent manner (K_d values are 81.5 and 66.3 nM for the Hsp70 and the NBD, respectively), and that P_i enhances the effect of the Mg^{2+} ion on the ADP binding (K_d values of 6.50 and 4.55 nM, respectively). Second, we compared the crystal structures of the ADP-bound Hsp70 NBDs with and without Mg^{2+} ion. In the ADP- and Mg^{2+} ion-bound NBD structure, the β-phosphate group of ADP is coordinated with one Mg^{2+} ion, which interacts with the side chains of Asp10, Glu175, and Asp199 from Hsp70, through four water molecules. Furthermore, the Mg^{2+} ion was also coordinated with one P_i molecule, which interacted with Lys71, Glu175, and Thr204. None of these residues is involved in ADP binding in the absence of Mg^{2+} ion. Third, we confirmed that the replacements of Asp10 and Asp199 with alanine residues reduced the Mg^{2+} ion-dependent high affinities for ADP, in both the presence and the absence of P_i. Therefore, we concluded that the Mg^{2+} ion connects ADP to Asp10 and Asp199, and P_i stabilizes the Mg^{2+} ion binding, which results in the slow release of ADP from Hsp70.

Results

Mg^{2+} ion increases the affinity of Hsp70 for ADP

To understand the mechanism of the P_i-dependent reduction in the ADP release rate,[22–26] we measured the dissociation constants of the Hsp70 NBD for ADP by ITC experiments. At first, the NBD protein and ADP were buffered with the P_i- and Mg^{2+} ion-containing buffer [20 mM Tris–HCl and 20 mM phosphate-K buffers (pH 8.0), containing 150 mM KCl, 5 mM $MgCl_2$, and 1 mM DTT], and the NBD protein solution was titrated with the ADP solution. As a result, we obtained the K_d value of 4.55 nM [Fig. 1(A)]. On the other hand, in the P_i-free and Mg^{2+} ion-containing buffer [20 mM Tris–HCl buffer (pH 8.0), containing 150 mM KCl, 5 mM $MgCl_2$, and 1 mM DTT], the K_d value increased to 66.3 nM [Fig. 1(B)]. As described above, a previous study showed that the presence of P_i reduced the release rate of ADP from Hsp70,[22] which is consistent with our results. Next, we performed ITC measurements in the P_i-containing and Mg^{2+} ion-free buffer [20 mM Tris–HCl and 20 mM phosphate-K buffers (pH 8.0), containing 150 mM KCl, 1 mM EDTA, and 1 mM DTT] and the P_i- and Mg^{2+} ion-free buffer [20 mM Tris–HCl buffer (pH 8.0), containing 150 mM KCl, 1 mM EDTA, and 1 mM DTT], and obtained the K_d values of 4.21 μM [Fig. 1(C)] and 4.61 μM [Fig. 1(D)], respectively. These results indicated that the Mg^{2+} ion removal reduces the affinity of the NBD for ADP more than the P_i removal, and that, in the absence of Mg^{2+} ion, the presence of P_i does not affect the ADP binding. Therefore, the Mg^{2+} ion increases the affinity of the Hsp70 NBD for ADP, and P_i enhances the effect of the Mg^{2+} ion.

The Mg^{2+} ion-dependent binding was also observed for the full-length Hsp70. In the P_i- and Mg^{2+} ion-containing buffer, the affinity of Hsp70 for ADP is remarkably high, with the K_d value of 6.50 nM [Fig. 1(E)]. In the P_i-free and Mg^{2+} ion-containing buffer, the affinity is reduced with the K_d value

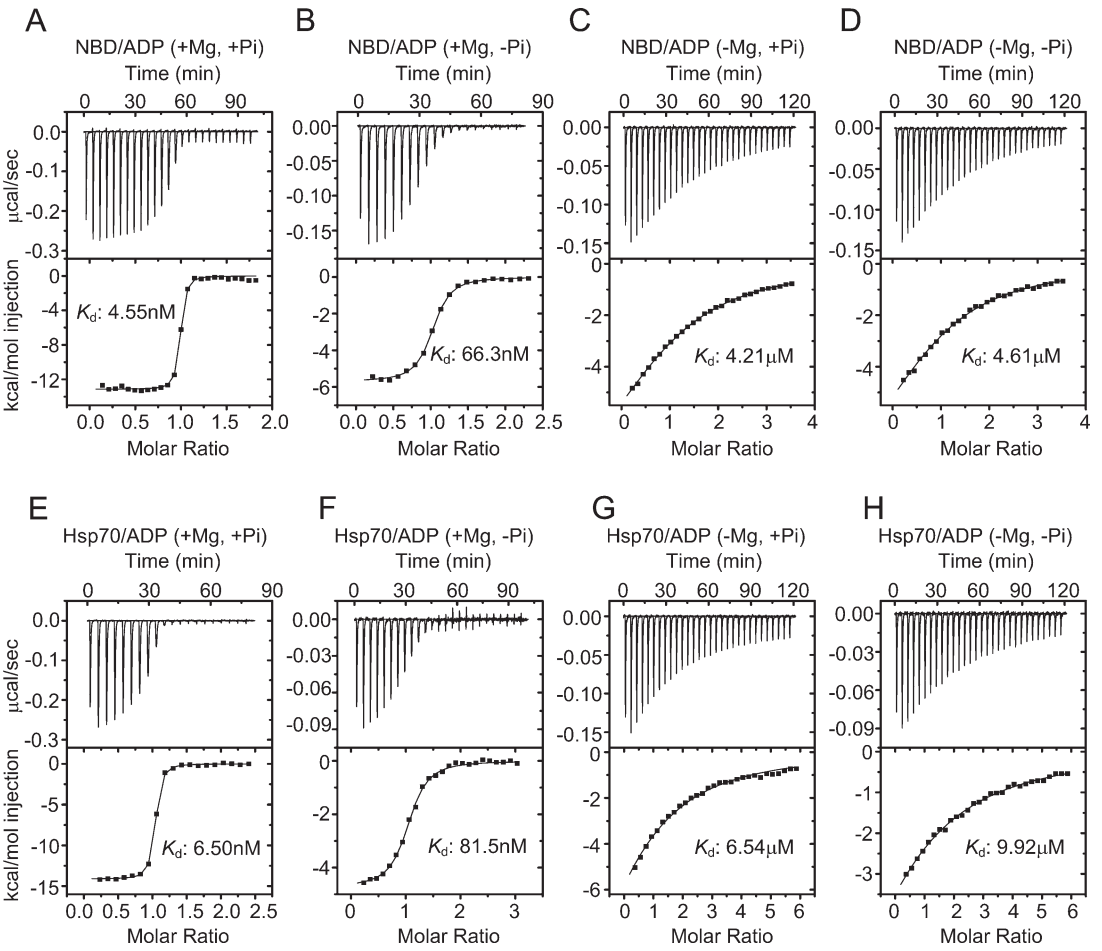

Figure 1. ITC analysis of the interactions of the Hsp70 NBD (A–D) and the full-length Hsp70 (E–H) with ADP, in the presence and absence of Mg^{2+} ion and P_i. (A) The NBD in the P_i- and Mg^{2+} ion-containing buffer. (B) The NBD in the P_i-free and Mg^{2+} ion-containing buffer. (C) The NBD in the P_i-containing and Mg^{2+} ion-free buffer. (D) The NBD in the P_i- and Mg^{2+} ion-free buffer. (E) Hsp70 in the P_i- and Mg^{2+} ion-containing buffer. (F) Hsp70 in the P_i-free and Mg^{2+} ion-containing buffer. (G) Hsp70 in the P_i-containing and Mg^{2+} ion-free buffer. (H) Hsp70 in the P_i- and Mg^{2+} ion-free buffer.

of 81.5 nM [Fig. 1(F)]. The removal of the Mg^{2+} ion reduces the affinity dramatically, and the K_d values in the P_i-containing and Mg^{2+} ion-free buffer and the P_i- and Mg^{2+} ion-free buffer were 6.54 μM [Fig. 1(G)] and 9.92 μM [Fig. 1(H)], respectively. Therefore, we concluded that Mg^{2+} ion increases the affinity of Hsp70 for ADP and that P_i promotes the effect of the Mg^{2+} ion. Note that the presence of both P_i and Mg^{2+} ion is physiological.

Crystal structures of the ADP-bound NBD

To determine how the Mg^{2+} ion increased the affinity of Hsp70 for ADP, we compared the crystal structures of the ADP-bound Hsp70 NBDs with and without the Mg^{2+} ion. At first, we expressed the Hsp70 NBD protein in *Escherichia coli* cells and purified it by column chromatography. To obtain the crystal of the ADP- and Mg^{2+} ion-bound NBD, ADP, $MgCl_2$, and phosphate-K buffer (pH 8.0) were added to the purified NBD sample, to final concentrations of 5 mM, 5 mM, and 20 mM, respectively. After cocrystallization, we collected the 1.75 Å data set of the ADP- and Mg^{2+} ion-bound NBD at a wavelength of 1.54 Å. In addition, for the crystallization of the ADP-bound and Mg^{2+} ion-free NBD, ADP and EDTA were added to the NBD sample to 5 mM final concentrations. After cocrystallization, we collected the 1.58 Å data set at a wavelength of 1 Å and the 1.95 Å data set at a wavelength of 1.54 Å. Both of the initial phases were determined by the molecular replacement method with the program MOLREP,[27] and the models were refined. Crystallographic data collection and refinement statistics are summarized in Table I. The overall refined structures of the ADP-bound NBD in the presence and absence of Mg^{2+} ion are presented in Figure 2(A,B), respectively.

We confirmed that both of the NBD structures contained the electron density of one ADP molecule and one K^+ ion [Fig. 2(C,D)]. The K^+ ions were confirmed by calculating the anomalous difference Fourier map [Fig. 2(E,F)]. In addition, Cl^- and Ca^{2+} ions were observed, but they were not located in the nucleotide-binding pocket. Moreover, we found the

Table I. *Crystallographic Data and Refinement Statistics*

	Mg^{2+} ion-bound	Mg^{2+} ion-free		Mg^{2+} ion-bound (Na)
Data collection				
Wave-length (Å)	1.54	1.00	1.54	1.00
Space group	$P2_12_12_1$	$P2_12_12_1$		$P2_12_12_1$
Unit cell				
a, *b*, *c* (Å)	45.73, 61.34, 142.65	45.86, 63.14, 144.22		46.11, 63.68, 143.53
α, β, γ (°)	90.0, 90.0, 90.0	90.0, 90.0, 90.0		90.0, 90.0, 90.0
Resolution (Å)	50–1.75 (1.81–1.75)[a]	50–1.58 (1.64–1.58)[a]	50–1.95 (2.02–1.95)[a]	50–1.65 (1.71–1.65)[a]
No. of measured reflections	448,081	271,116	317,432	315,115
No. of unique reflections	72,057	56,315	57,853	50,891
Redundancy	6.21	4.81	5.49	6.19
Completeness (%)	92.5 (87.7)[a]	96.5 (90.5)[a]	97.3 (82.9)[a]	98.1 (85.7)[a]
I/σ (I)	10.1 (3.60)[a]	20.9 (3.20)[a]	21.4 (2.33)[a]	28.8 (2.39)[a]
R_{sym}[b] (%)	12.9 (52.3)[a]	6.7 (31.8)[a]	7.1 (37.6)[a]	5.9 (37.4)[a]
Refinement statistics				
Resolution (Å)	20–1.75	20–1.58		20–1.65
No. of reflections	36,093	53,369		48,203
R_{work}/R_{free}[c] (%)	18.9/21.3	18.6/20.8		18.6/21.8
RMSD bond lengths (Å)	0.013	0.010		0.011
RMSD bond angles (°)	1.412	1.305		1.334
Average isotropic *B*-value (Å^2)	26.3	18.2		23.0
Ramachandran plot (%)				
Most favored regions	92.3	93.2		93.2
Additional allowed regions	7.7	6.8		6.8
Generously allowed regions	0	0		0
Disallowed regions	0	0		0
PDB code	3AY9	3ATV		3ATU

[a] Statistics for the highest resolution shell are given in parentheses.
[b] $R_{sym} = \Sigma|I - \langle I\rangle|/\Sigma I$, where I is the observed intensity of reflections.
[c] R_{work}, $R_{free} = \Sigma|F_{obs} - F_{calc}|/\Sigma F_{obs}$, where the crystallographic R-factor is calculated including and excluding refinement reflections. In each refinement, free reflections consist of 5% of the total number of reflections.

electron densities of one Mg^{2+} ion and one P_i molecule in the nucleotide-binding pocket of the ADP- and Mg^{2+} ion-bound NBD [Fig. 2(C)]. The overall structures of the ADP-bound NBDs with and without Mg^{2+} ion were quite similar, with a root mean square deviation (RMSD) of 0.37 Å. Therefore, the absence of Mg^{2+} ion and P_i does not affect the overall structure of the NBD.

Nucleotide-binding pocket of the ADP-bound NBD

Next, we compared the nucleotide-binding pockets in the ADP-bound NBD structures with and without Mg^{2+} ion. The nucleotide-binding pocket is surrounded by the four subdomains, IA (residues 1–39, 116–188, and 361–384), IB (residues 40–115), IIA (residues 189–228 and 307–360), and IIB (residues 229–306) of the Hsp70 NBD [Fig. 2(A,B)]. In both of the present structures, the ADP molecule is bound in the pocket, interacting with subdomains IA, IIA, and IIB. The adenosine moiety interacts with the side chains of Glu268, Lys271, and Ser275 from subdomain IIB. The α-phosphate group interacts with the main-chain amide group of Gly339 from subdomain IIA, and the β-phosphate group is associated with the main and side chains of Thr13 and Thr14 and main-chain of Tyr15. Consequently, the modes of the direct interactions between the NBD protein and the ADP molecule in the ADP-bound states with and without Mg^{2+} ion are almost the same [Fig. 3(A,B)].

Additionally, the ADP- and Mg^{2+} ion-bound NBD interacts indirectly with ADP, through one Mg^{2+} ion. The Mg^{2+} ion forms a coordinate bond with the β-phosphate group of ADP. Furthermore, the Mg^{2+} ion is coordinated with one P_i molecule and four water molecules [Fig. 3(C)]. Two of the water molecule hydrogen bonds with the side chain of Asp10, another water molecule hydrogen bonds with the side chain of Asp199 (subdomain IIA), and the other water molecule hydrogen bonds with the side chains of Glu175 (subdomain IA) and Asp199 [Fig. 3(C)]. These interactions are not observed in the ADP-bound NBD without Mg^{2+} ion. The interactions of the β-phosphate group of ADP with Asp10, Glu175, and Asp199, through the Mg^{2+} ion and the four water molecules are likely to form the basis of the higher affinity of Hsp70 for ADP than in the absence of Mg^{2+} ion. Moreover, the P_i molecule, which is coordinated with the Mg^{2+} ion, interacts with the side chains of Lys71 (subdomain IB), Glu175 (subdomain IA), and Thr204 (subdomain IIA). Therefore, it

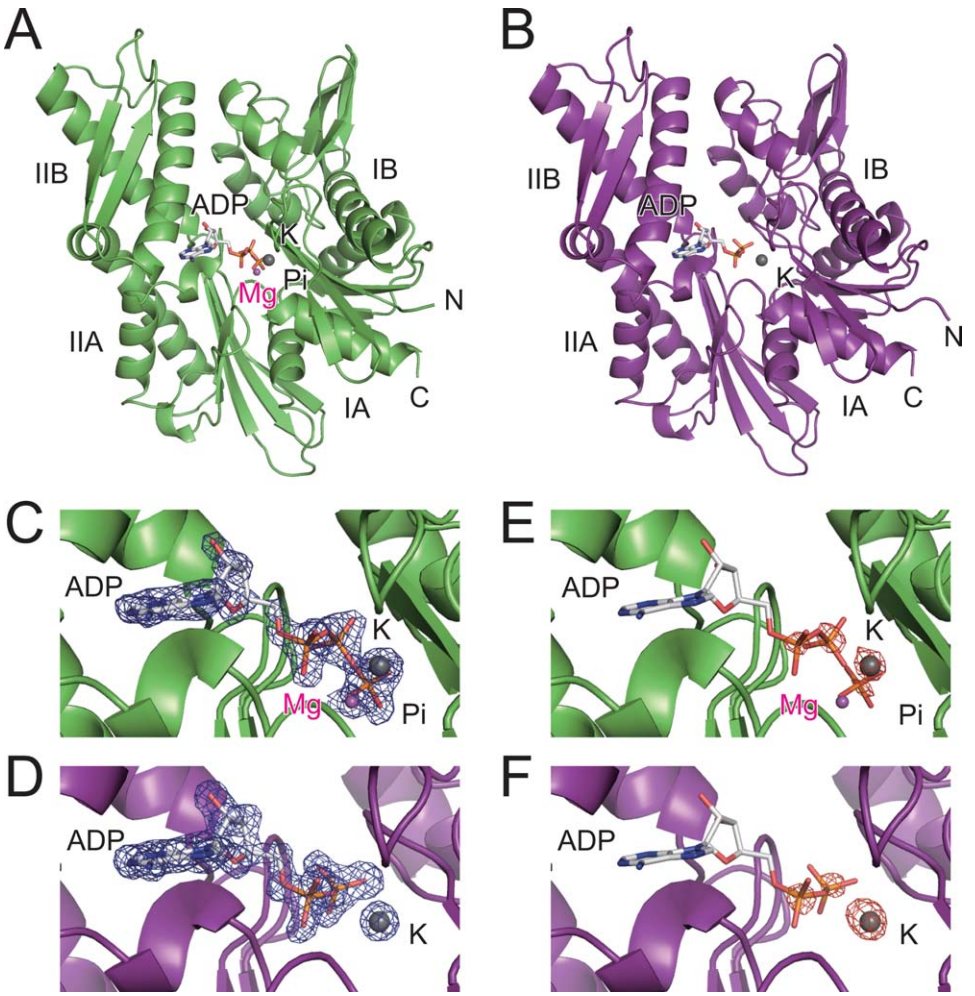

Figure 2. Crystal structures of the ADP-bound NBD, with and without Mg^{2+} ion. (A) Crystal structure of the ADP- and Mg^{2+} ion-bound NBD (green). The stick models represent ADP and P_i, and the balls represent Mg^{2+} (magenta) and K^+ (gray) ions. (B) Crystal structure of the ADP-bound and Mg^{2+} ion-free NBD (purple). The stick model represents ADP, and the gray ball represents the K^+ ion. (C) The nucleotide-bound pocket of the ADP- and Mg^{2+} ion-bound NBD. The electron density indicates the $F_o - F_c$ omit map (3σ level). (D) The nucleotide-bound pocket in the ADP-bound and Mg^{2+} ion-free NBD. The electron density indicates the $F_o - F_c$ omit map (3σ level). (E) Anomalous difference Fourier map (4σ level) in the nucleotide-binding pocket of the ADP- and Mg^{2+} ion-bound NBD. (F) Anomalous difference Fourier map (4σ level) in the nucleotide-binding pocket of the ADP-bound and Mg^{2+} ion-free NBD. Molecular graphics were generated and rendered with the PyMOL program (DeLano Scientific, Palo Alto, CA).

is indicated that the promoting effect of P_i is due to the fixation of the Mg^{2+} ion in the site.

One K^+ ion, which was derived from the purification buffer, is coordinated with the β-phosphate group of ADP and is also directly coordinated with the side chain of Asp10 (subdomain IA) and the main chain of Tyr15 [subdomain IA; Fig. 3(C)]. On the other hand, in the ADP-bound and Mg^{2+} ion-free NBD, one K^+ ion, which was provided by the crystallization solution, is directly coordinated with the α–β bridging oxygen atom of ADP, the side chain of Asp10, and the main chain of Tyr15 [Fig. 3(D)]. Although the K^+ ions associate with the NBD and ADP independently of the Mg^{2+} ion, the Mg^{2+} ion shifts the orientation of the β-phosphate group of ADP, so that the K^+ ion is directly coordinated with the β-phosphate group in the ADP- and Mg^{2+} ion-bound NBD [Fig. 3(C)].

The effects of K^+ and Na^+ ions on ADP binding

In the cytosol, Hsp70 requires a K^+ ion, rather than a Na^+ ion, for its ATP hydrolysis and refolding activities.[28,29] The major reason may be that the K^+ ion is larger than the Na^+ ion, and thus, appropriately shifts the orientation of the triphosphate group of ATP, to facilitate ATP hydrolysis by Hsp70. However, it has also been reported that the K_d value of bovine Hsc70 for ADP in the presence of Na^+ ion is the same as that in the presence of K^+ ion.[28] In this context, we examined the effects of K^+ and Na^+ ions on the ADP binding.

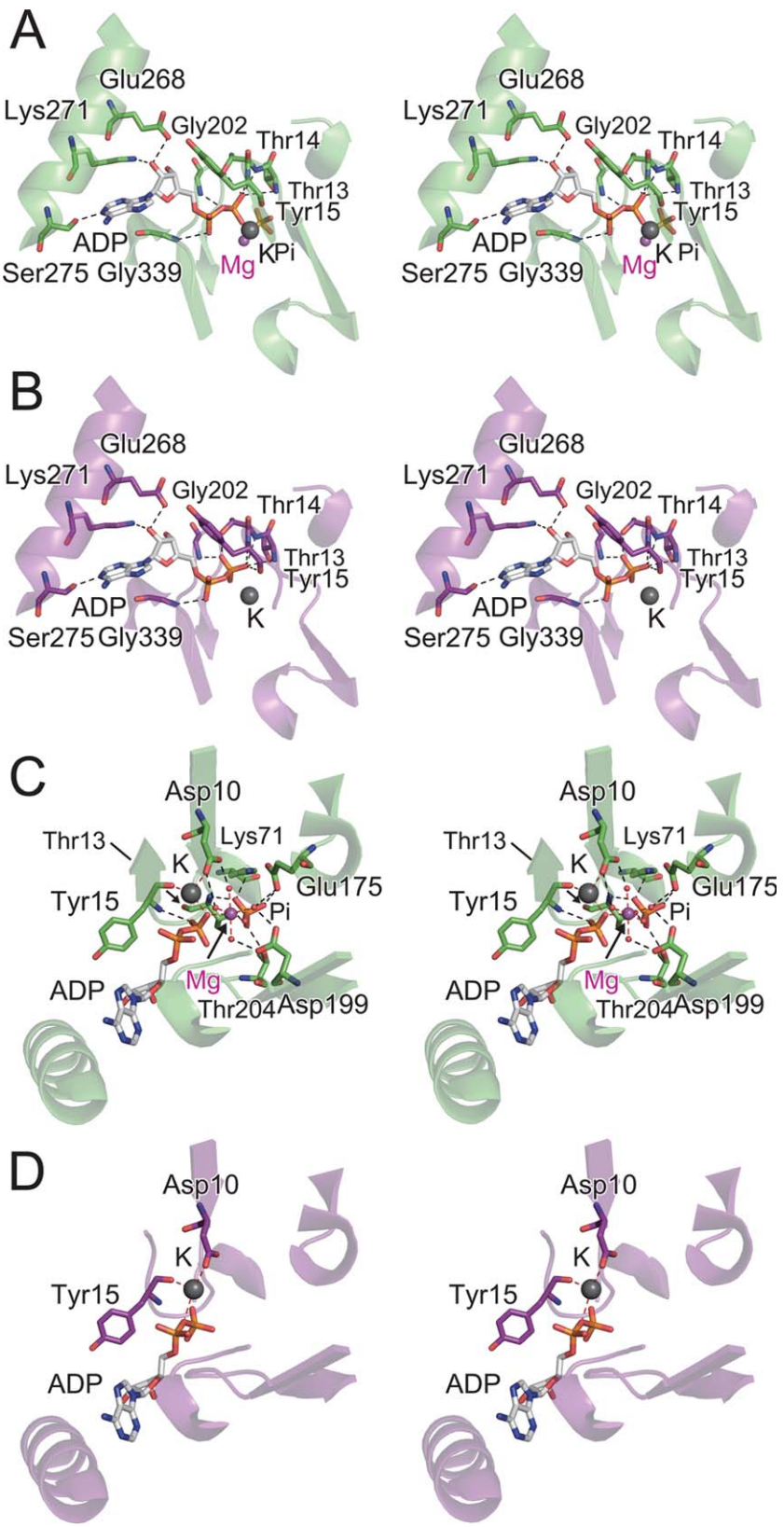

Figure 3. Interactions between the NBD and ADP, in the presence and absence of Mg^{2+} ion. (A) The direct interactions in the presence of Mg^{2+} ion (stereo view). (B) The direct interactions in the absence of Mg^{+} ion (stereo view). (C) The indirect interactions in the presence of Mg^{2+} ion (stereo view). (D) The indirect interactions in the absence of Mg^{2+} ion (stereo view). The interacting residues are shown as stick models, with the translucent ribbon model of the NBD in green (A and C) and purple (B and D). ADP and P_i are also shown as stick models. The Mg^{2+} ion is colored magenta, and the K^{+} ion is represented by a gray ball. Water molecules are shown as red dots. Black and red dashed lines represent hydrogen bonds and coordinate bonds, respectively.

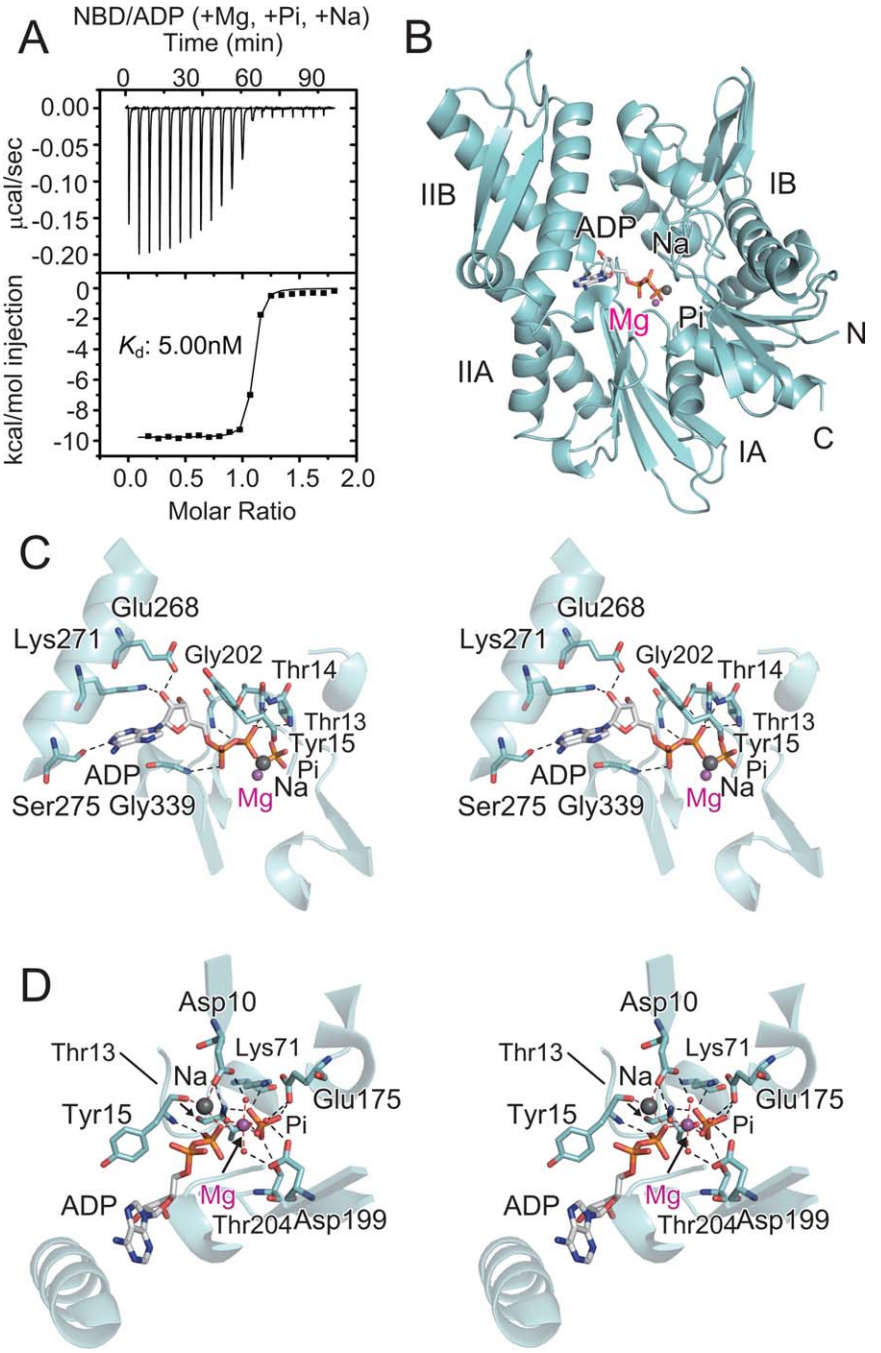

Figure 4. Interactions between the NBD and ADP, in the presence of Na^+ ion. (A) ITC analysis of the interactions between the NBD and ADP, in buffer containing Pi-, Mg^{2+}, and Na^+ ions. (B) Crystal structure of the ADP- and Mg^{2+} ion-bound NBD containing Na^+ ion. (C) The direct interactions between the NBD and ADP (stereo view). (D) The indirect interactions between the NBD and ADP (stereo view). The interacting residues are shown as stick models, with the ribbon model of the NBD in cyan. ADP and P_i are also shown as stick models. The Mg^{2+} ion is colored magenta, and the Na^+ ion is represented by a gray ball. Water molecules are shown as red dots. Black and red dashed lines represent hydrogen bonds and coordinate bonds, respectively.

First, we performed ITC experiments to measure the affinity of the NBD for ADP in 20 mM Tris–HCl and 20 mM phosphate–Na buffers (pH 8.0), containing 150 mM NaCl, 5 mM $MgCl_2$, and 1 mM DTT and obtained the K_d value of 5.00 nM [Fig. 4(A)], which is nearly equal to the K_d value of 4.55 nM for the NBD in the KCl-containing buffer [Fig. 1(A)]. Next, we purified the NBD in the NaCl-containing buffer and crystallized the ADP- and Mg^{2+} ion-bound NBD without K^+ ion. A 1.65 Å native data set was collected, and the initial phase was determined by the same method as for the ADP-

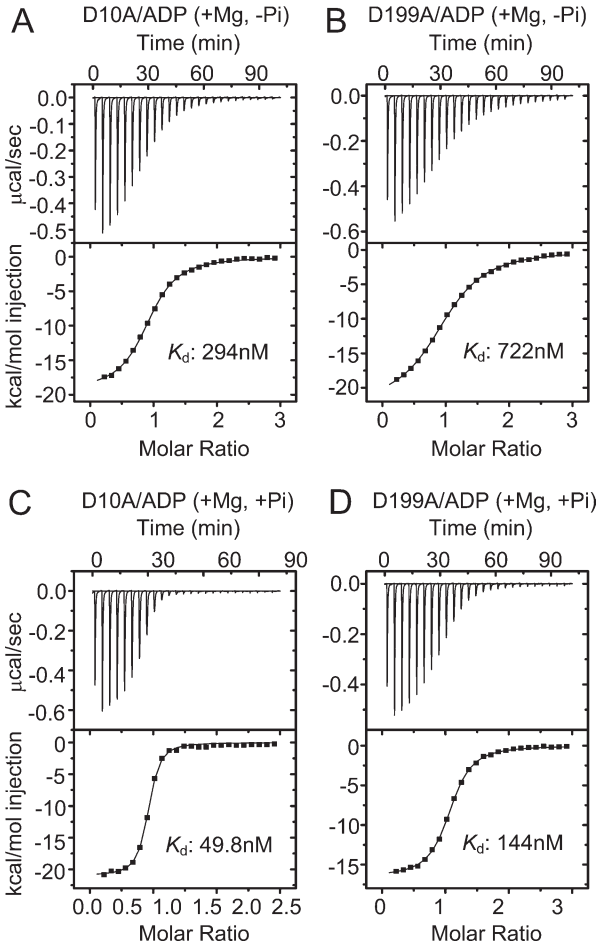

Figure 5. ITC analysis of the interactions of the NBD mutants with ADP. (A) The D10A mutant in the P_i-free and Mg^{2+} ion-containing buffer. (B) The D199A mutant in the P_i-free and Mg^{2+} ion-containing buffer. (C) The D10A mutant in the P_i- and Mg^{2+} ion-containing buffer. (D) The D199A mutant in the P_i- and Mg^{2+} ion-containing buffer.

bound NBD structures in the presence of K^+ ions. The overall structure, shown in Figure 4(B), is quite similar to the ADP- and Mg^{2+} ion-bound NBD containing K^+ ion, with an RMSD of 0.39 Å, and the direct interaction between the NBD and ADP [Fig. 4(C)] is the same as that in the presence of K^+ ion. Furthermore, the Na^+ ion, which is derived from the purification buffer, is coordinated with Tyr15, Asp10, and the β-phosphate group of ADP and is located in the same position as the K^+ ion, so the indirect interaction is also the same. Therefore, although the K^+ ion is indispensable for the ATP hydrolysis and refolding activities of Hsp70, the K^+ ion can be replaced with the Na^+ ion, with respect to ADP binding.

The replacement of Asp10 or Asp199 in Hsp70 reduces the affinity for ADP

To examine the contributions of Asp10 and Asp199, which interact with the Mg^{2+} ion but lack interactions with P_i, we prepared the D10A and D199A mutants of the NBD, and performed ITC experiments to measure their affinity for ADP in the absence and presence of P_i (Fig. 4). First, in the P_i-free and Mg^{2+} ion-containing ITC buffer, the D10A and D199A mutations reduced the binding affinity for ADP by about 5- and 12-fold, respectively, as compared with the wild-type NBD under the same conditions; the K_d value of the D10A mutant was 294 nM [Fig. 5(A)] and that of the D199A mutant was 722 nM [Fig. 5(B)]. Consequently, these two residues are essential for the high affinity for ADP in the absence of P_i. Furthermore, in the P_i- and Mg^{2+} ion-containing ITC buffer, the mutations still reduced the binding affinity for ADP by about 10- and 30-fold, respectively, as compared with the wild type; the K_d value of the D10A mutant was 49.8 nM [Fig. 5(C)] and that of the D199A mutant was 144 nM [Fig. 5(D)]. These results confirmed that both Asp10 and Asp199 contribute to the high affinity for ADP, even in the presence of P_i. Therefore, the entire network of interactions shown in Figure 3(C) is required for the high affinity for ADP, with the nM-level dissociation constant.

Discussion

The rate of ADP dissociation from Hsp70 is reportedly slow, and is further reduced by P_i.[22–26] In this study, to investigate the ADP binding to Hsp70 in detail, we performed ITC measurements under various buffer conditions, and found that Mg^{2+} ion greatly increases the affinity of Hsp70 for ADP. Although the overall structures of the ADP-bound NBD with and without Mg^{2+} ion are almost the same, the ADP and Mg^{2+} ion-bound NBD contains one Mg^{2+} ion, which are coordinated with the β-phosphate group of ADP. The Mg^{2+} ion is also coordinated with P_i and four water molecules, which hydrogen bond with the side chains of Asp10, Glu175, and Asp199. Actually, in the absence of P_i and the presence of Mg^{2+} ion, the affinities of the D10A and the D199A mutants for ADP are about 5- and 12-fold lower than that of the wild type, respectively. Therefore, the Mg^{2+} ion is required for the high affinity for ADP.

In the presence of Mg^{2+} ion, P_i increases the affinity of the NBD and the full-length Hsp70 for ADP by about 12-fold, which is consistent with the previous reports.[26] In the ADP- and Mg^{2+} ion-bound NBD structure, P_i interacts with the Mg^{2+} ion and the side-chains of Lys71, Glu175, and Thr204. Through these interactions, the P_i fixes the Mg^{2+} ion, thus enhancing the effect of the Mg^{2+} ion on the ADP binding. Furthermore, in the presence of Mg^{2+} ion, the addition of P_i increases the affinities of the D10A and D199A mutants for ADP, whereas the addition of P_i does not increase the affinity of the wild type in the absence of Mg^{2+} ion. These results suggest that the Asp10 and Asp199 residues from

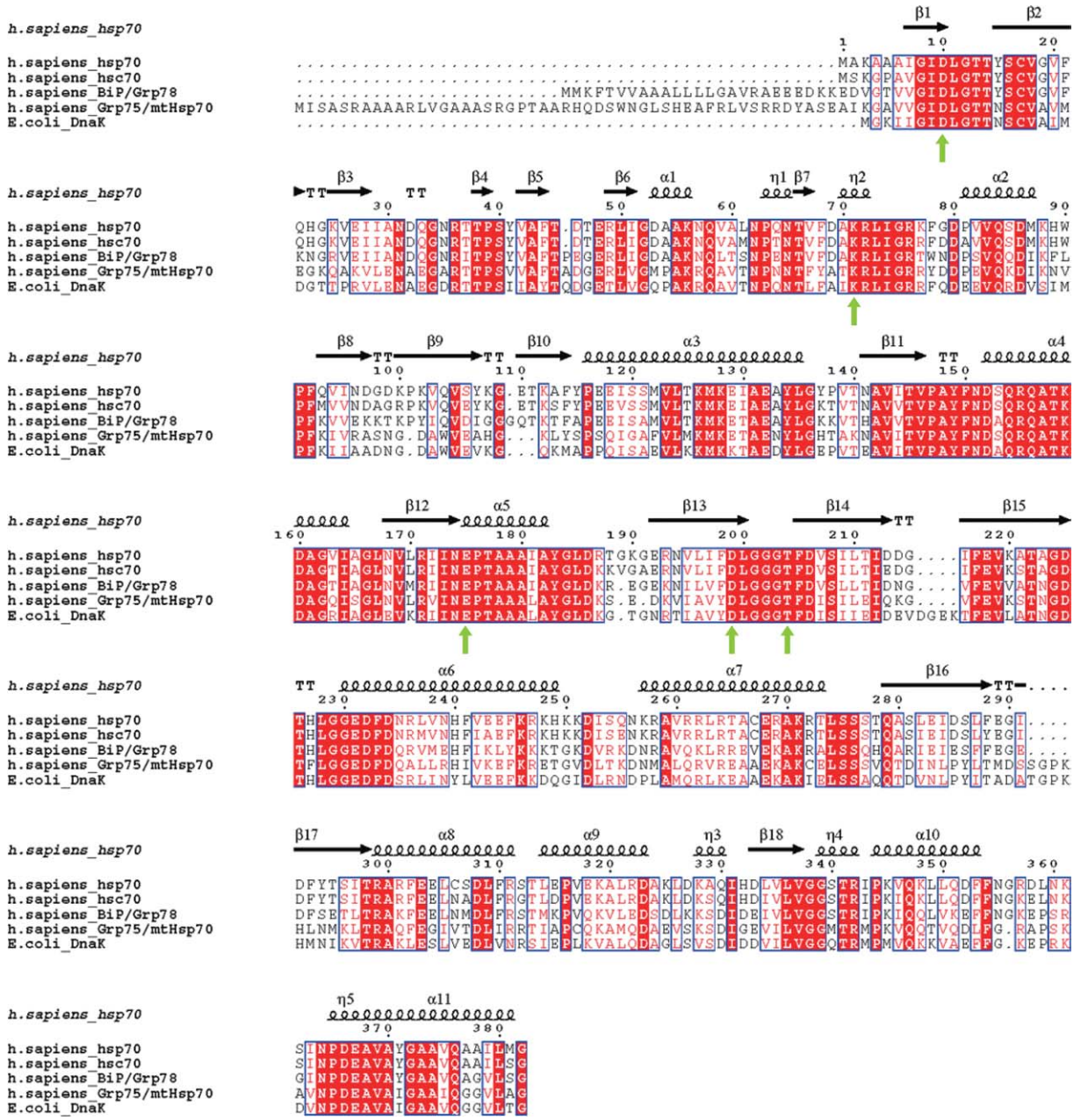

Figure 6. Amino acid sequence alignment of the NBDs of five Hsp70-family proteins. Sequences are the NBDs of human (*Homo sapiens*) Hsp70 (NCBI Gene ID: 3303), Hsc70 (NCBI Gene ID: 3312), Bip/Grp78 (NCBI Gene ID: 3309), Grp75/mtHsp70 (NCBI Gene ID: 3313), and *E. coli* DnaK (NCBI Gene ID: 944750). Above the sequences, the secondary structures of human Hsp70 NBD are indicated. The residues involved in the Mg^{2+} ion-mediated network are indicated by green arrows.

Hsp70 and the P_i cooperatively work to fasten the Mg^{2+} ion. Consequently, the Mg^{2+} ion-mediated network, including the P_i and water molecules and the Asp residues, is important for the high affinity of Hsp70 for ADP. Furthermore, not only Asp10 and Asp199 but also Lys71, Glu175, and Thr204, which interact with P_i, are conserved among the Hsp70-family proteins, including the other human Hsp70 isoforms and DnaK from *E. coli* (Fig. 6). Therefore, the high ADP affinity due to the Mg^{2+} ion-mediated network is likely to be a common feature of the Hsp70-family proteins.

The crystal structure of the ATP-bound Hsc70 NBD in the pre-ATP hydrolysis state has been reported.[30] In this state, the β- and γ-phosphate groups of ATP interact with one Mg^{2+} ion, and the water molecule that interacts with the side chain of Lys71 is poised to attack the γ-phosphate group of ATP.[31] The Mg^{2+} ion and the residues that are involved in the Mg^{2+} ion-mediated network are located in the same positions as those in the ADP- and Mg^{2+} ion-bound NBD structure. Moreover, the mutations of the residues involved in the Mg^{2+} ion-mediated network reportedly impaired the ATP

Table II. *Summary of the ITC Experiments*

Cell	Syringe	Buffer condition	N	K_d (nM)	ΔH (cal/mol)	ΔS (cal/mol/°)
Hsp70 NBD	ADP	+Pi, +Mg, +K	0.969 ± 0.004	4.55 ± 0.64	−13.3 ± 0.1	−6.50 ± 0.40
Hsp70 NBD	ADP	−Pi, +Mg, +K	0.971 ± 0.014	66.3 ± 14.1	−5.53 ± 0.24	14.5 ± 1.3
Hsp70 NBD	ADP	+Pi, −Mg, +K	0.997 ± 0.066	4210 ± 970	−9.91 ± 0.57	−8.50 ± 2.45
Hsp70 NBD	ADP	−Pi, −Mg, +K	0.988 ± 0.005	4610 ± 690	−9.33 ± 0.93	−6.86 ± 3.44
Hsp70 FL	ADP	+Pi, +Mg, +K	1.02 ± 0.03	6.50 ± 1.18	−14.8 ± 1.0	−12.3 ± 3.1
Hsp70 FL	ADP	−Pi, +Mg, +K	1.04 ± 0.01	81.5 ± 8.8	−5.12 ± 0.19	15.3 ± 0.4
Hsp70 FL	ADP	+Pi, −Mg, +K	0.958 ± 0.018	6540 ± 230	−17.5 ± 0.5	−35.1 ± 1.6
Hsp70 FL	ADP	−Pi, −Mg, +K	1.07 ± 0.01	9920 ± 610	−14.9 ± 1.2	−27.0 ± 4.1
NBD D10A	ADP	+Pi, +Mg, +K	0.898 ± 0.009	49.8 ± 2.4	−21.1 ± 0.1	−37.4 ± 0.4
NBD D10A	ADP	−Pi, +Mg, +K	0.936 ± 0.014	294 ± 18	−18.7 ± 0.4	−32.9 ± 1.4
NBD D199A	ADP	+Pi, +Mg, +K	1.04 ± 0.01	144 ± 10	−16.9 ± 0.2	−25.2 ± 0.6
NBD D199A	ADP	−Pi, +Mg, +K	1.04 ± 0.02	722 ± 17	−22.4 ± 0.1	−46.9 ± 0.2
Hsp70 NBD	ADP	+Pi, +Mg, +Na	1.09 ± 0.04	5.00 ± 1.86	−10.0 ± 0.2	4.65 ± 1.37

Each experiment was repeated three times.

hydrolysis activity and the ATP-dependent conformational change of Hsp70,[32,33] and these residues are also essential for its chaperone activity. Thus, the formation of the Mg^{2+} ion-mediated network in the ADP-bound NBD results unavoidably from the ATP hydrolysis by Hsp70. For the ADP–ATP exchange reaction of Hsp70, the high ADP affinity due to the Mg^{2+}-mediated network might be an obstacle. However, nucleotide-exchange factors are present in all organisms, and they facilitate the ADP–ATP exchange reaction. The reported structures of Hsp70 (fragment) in complex with exchange factors, such as GrpE, BAG proteins, HspBP1, and Hsp110, indicate that the exchange factors disrupt the Mg^{2+} ion-mediated network of the ADP-bound NBD. Therefore, Hsp70 can efficiently function as a molecular chaperone.

Materials and Methods

Protein expression

The construction of the expression plasmids for the NBD (residues 1–388) and the full-length of human Hsp70, as N-terminal fusions with a His-tag and a TEV protease cleavage site, was described previously.[18] The mutations were introduced by QuickChange (Stratagene) mutagenesis and were verified by DNA sequencing. The wild-type and mutant proteins were expressed in *E. coli* strain Rosetta2 (DE3) cells induced by 0.5 mM isopropyl-1-thio-β-D-galactopyranoside.

ITC measurement

For ITC measurements, protein samples were prepared as described previously.[18] Briefly, the wild type and mutants of the NBD and full-length Hsp70 proteins were expressed in *E. coli* cells and purified with a HisTrap column (GE Healthcare). After cleavage of the His-tag by TEV protease, the proteins were purified by chromatography on a HisTrap column, a HiTrap Blue column (GE Healthcare), a Mono Q column (GE Healthcare), and a Superdex 200 column (GE Healthcare). The NBD and full-length Hsp70 samples purified by this method are in the nucleotide-free state, as confirmed by HPLC.[34] ITC measurements were performed at 25°C with a Microcal VP-ITC calorimeter (MicroCal, Northhampton, MA). For each injection, a 5 μL portion of the ADP solution in the syringe was injected into the protein solution in the cell, at 240-s intervals. The data were processed with the MicroCal Origin software, version 7.0. Each measurement was repeated three times, and the averages and the standard deviations were evaluated. All results are summarized in Table II.

Purification and crystallization of the Hsp70 NBD

The cells were suspended in 20 mM Tris–HCl buffer (pH 8.0), containing 500 mM NaCl and 5 mM imidazole, and lysed by sonication. The lysate was clarified by centrifugation and then loaded on a HisTrap column, which was eluted with an imidazole gradient. Next, His-tagged TEV protease was added to the protein solution, and the sample was dialyzed against 20 mM Tris–HCl buffer (pH 8.0), containing 300 mM NaCl. The tag-cleaved NBD sample was loaded on the HisTrap column again, to remove the TEV protease and the cleaved His-tag. Subsequently, the NBD sample was dialyzed against 20 mM Tris–HCl buffer (pH 8.0), containing 300 mM NaCl and 5 mM EDTA, overnight at 4°C and then, dialyzed against 20 mM Tris–HCl buffer (pH 8.0), containing 50 mM NaCl and 5 mM EDTA. The NBD sample was then purified by chromatography on a Resource Q column (GE Healthcare). Finally, the NBD sample was loaded on a Superdex 200 column, which was eluted with 20 mM Tris–HCl buffer (pH 8.0), containing 150 mM NaCl and 1 mM DTT. Additionally, for the crystallization of the ADP- and Mg^{2+} ion-bound NBD containing K^+ ion, the sample buffer was exchanged to Tris–HCl buffer (pH 8.0),

Table III. *Anomalous Difference Peaks*

Mg^{2+} ion-bound NBD		Mg^{2+} ion-free NBD	
Peak height (σ)	Atom assignment	Peak height (σ)	Atom assignment
8.15	Sulfur of Cys17	13.51	K^+ ion
8.06	K^+ ion	7.15	Pα of ADP
7.72	Cl^- ion	7.12	Sulfur of Met127
7.30	Ca^{2+} ion	7.06	Sulfur of Cys17
7.08	Sulfur of Cys267	6.54	Pβ of ADP
7.06	Pβ of ADP	6.28	Sulfur of Cys306
6.98	Sulfur of Met122	5.97	Cl^- ion
5.94	Sulfur of Met127	5.69	Solvent
5.77	Pα of ADP	5.43	Sulfur of Met122
5.62	P of Pi	5.41	Sulfur of Cys267
5.61	Sulfur of Met381		
5.22	Sulfur of Cys306		

Only peaks above 5σ are listed.

containing 150 mM KCl and 1 mM DTT, by gel-filtration chromatography (Superdex 200 column).

The NBD sample was concentrated to about 10 mg/mL. To obtain the crystal of the ADP- and Mg^{2+} ion-bound NBD containing K^+ ion (Crystal 1), the protein sample was mixed with ADP, $MgCl_2$, and phosphate-K buffer (pH 8.0) at final concentrations of 5 mM, 5 mM, and 20 mM, respectively and crystallized by the sitting-drop vapor-diffusion method at 293 K, against the reservoir solution [0.1 M Bis–Tris buffer (pH 5.5), containing 0.05 M $CaCl_2$ and 30 % polyethylene glycol monomethyl ether 500]. The crystal belonged to the space group $P2_12_12_1$, with unit-cell parameters $a = 45.73$ Å, $b = 61.34$ Å, $c = 142.65$ Å, $\alpha = \beta = \gamma = 90.00°$. To obtain the crystal of the ADP-bound and Mg^{2+}-free NBD (Crystal 2), the protein sample was mixed with ADP and EDTA to final concentrations of 5 mM, and crystallized by the same method, against the reservoir solution [0.1 M Bis–Tris buffer (pH 5.5), containing 0.25 M KNO_3 and 25% polyethylene glycol 3350]. The crystal belonged to the space group $P2_12_12_1$, with unit-cell parameters $a = 45.86$ Å, $b = 63.14$ Å, $c = 144.22$ Å, $\alpha = \beta = \gamma = 90.00°$. To obtain the crystal of the ADP- and Mg^{2+} ion-bound NBD containing Na^+ ion (Crystal 3), the protein sample was mixed with ADP and $MgCl_2$ to final concentrations of 5 mM and crystallized by the same method, against the reservoir solution [0.1 M HEPES buffer (pH 7.0), containing 0.15 M $MgCl_2$ and 30% polyethylene glycol monomethyl ether 500]. The crystal belonged to the space group $P2_12_12_1$, with unit-cell parameters $a = 46.11$ Å, $b = 63.68$ Å, $c = 143.53$ Å, $\alpha = \beta = \gamma = 90.00°$.

Data collection and structure determination

Crystal 1 was directly flash cooled in liquid nitrogen. The diffraction data were measured at the BL-17A beamline of the Photon Factory (Tsukuba, Japan) at a wavelength of 1.54 Å. Crystal 2 was cryoprotected with 15% glycerol in the reservoir solution and was flash cooled in liquid nitrogen. The diffraction data were collected at the BL26B2 beamline of SPring-8 (Harima, Japan) at wavelengths of 1.00 and 1.54 Å. Crystal 3 was cryoprotected with 15% glycerol in the reservoir solution and was flash cooled in liquid nitrogen. The diffraction data were collected at the BL26B2 beamline of SPring-8 at a wavelength of 1.00 Å. All X-ray diffraction data were processed using the HKL2000 program.[35] The initial phases were determined by the molecular replacement method with the program MOLREP,[27] using the structure of the human Hsp70 NBD in the AMPPNP-bound state (PDB ID: 2E8A)[34] as the search model. Next, we used the CNS programs[36] and the Refmac5 program[37] to refine the structures, and modified the protein models with the TURBO-FRODO program (http://www.afmb.univ-mrs.fr/-TURBO-) and the Coot program.[38] The ADP, P_i, and PEG molecules and the Mg^{2+}, Na^+, K^+, Cl^-, and Ca^{2+} ions were added into the electron densities, which were visible in the $F_o - F_c$ map. All of the numbers and distances of the coordinate bonds between the metal ions and the oxygen atoms are appropriate,[39] and the anomalous signals of the K^+, Cl^-, and Ca^{2+} ions were observed in the anomalous difference Fourier maps. Anomalous difference peaks in Crystals 1 and 2 are listed in Table III. Crystal 3 contained P_i, which was probably derived from the small amount of P_i in the ADP sample, as P_i was not added to the NBD sample for purification and crystallization. The final refined model of the ADP- and Mg^{2+} ion-bound NBD containing K^+ ion achieved an R/R_{free} of 18.9/21.3, that of the ADP-bound and Mg^{2+} ion-free NBD achieved an R/R_{free} of 18.6/20.8, and that of the ADP- and Mg^{2+} ion-bound NBD containing Na^+ ion achieved an R/R_{free} of 18.6/21.8. The final models had no Ramachandran violations, as confirmed by PROCHECK.[40] The atomic coordinates and structure factors have been deposited in the Protein Data Bank (accession codes: 3AY9 for the structure of the ADP- and Mg^{2+} ion-bound NBD containing K^+ ion, 3ATV for the structure of the ADP-bound and Mg^{2+}-free NBD, and 3ATU for the structure of the ADP- and Mg^{2+} ion-bound NBD containing Na^+ ion).

Acknowledgments

The authors thank Dr. M. Shida for discussions on the high affinity of Hsp70 for ADP. The authors are grateful to Drs. T. Kasai, T. Terada, and T. Sengoku for their advice on the ITC measurements, protein purification, and the calculating anomalous difference Fourier map, respectively, and also to Drs. T. Umehara, H. Niwa, and R. Akasaka, and the beamline staff at BL26B2 at SPring-8 (Hyogo, Japan) for X-ray data collection.

References

1. Bukau B, Horwich AL (1998) The Hsp70 and Hsp60 chaperone machines. Cell 92:351–366.
2. Bukau B, Weissman J, Horwich A (2006) Molecular chaperones and protein quality control. Cell 125: 443–451.
3. Young JC, Agashe VR, Siegers K, Hartl FU (2004) Pathways of chaperone-mediated protein folding in the cytosol. Nat Rev Mol Cell Biol 5:781–791.
4. Mayer MP (2010) Gymnastics of molecular chaperones. Mol Cell 39:321–331.
5. Wilbanks SM, Chen L, Tsuruta H, Hodgson KO, McKay DB (1995) Solution small-angle X-ray scattering study of the molecular chaperone Hsc70 and its subfragments. Biochemistry 34:12095–12106.
6. Johnson ER, McKay DB (1999) Mapping the role of active site residues for transducing an ATP-induced conformational change in the bovine 70-kDa heat shock cognate protein. Biochemistry 38:10823–10830.
7. Mapa K, Sikor M, Kudryavtsev V, Waegemann K, Kalinin S, Seidel CA, Neupert W, Lamb DC, Mokranjac D (2010) The conformational dynamics of the mitochondrial Hsp70 chaperone. Mol Cell 38:89–100.
8. Liu Q, Hendrickson WA (2007) Insights into Hsp70 chaperone activity from a crystal structure of the yeast Hsp110 Sse1. Cell 131:106–120.
9. Walsh P, Bursac D, Law YC, Cyr D, Lithgow T (2004) The J-protein family: modulating protein assembly, disassembly and translocation. EMBO Rep 5:567–571.
10. Jiang J, Maes EG, Taylor AB, Wang L, Hinck AP, Lafer EM, Sousa R (2007) Structural basis of J cochaperone binding and regulation of Hsp70. Mol Cell 28:422–433.
11. Chang YW, Sun YJ, Wang C, Hsiao CD (2008) Crystal structures of the 70-kDa heat shock proteins in domain disjoining conformation. J Biol Chem 283: 15502–15511.
12. Bertelsen EB, Chang L, Gestwicki JE, Zuiderweg ER (2009) Solution conformation of wild-type *E.coli* Hsp70 (DnaK) chaperone complexed with ADP and substrate. Proc Natl Acad Sci USA 106:8471–8476.
13. Jiang J, Prasad K, Lafer EM, Sousa R (2005) Structural basis of interdomain communication in the Hsc70 chaperone. Mol Cell 20:513–524.
14. Hohfeld J, Jentsch S (1997) GrpE-like regulation of the hsc70 chaperone by the anti-apoptotic protein BAG-1. EMBO J 16:6209–6216.
15. Harrison CJ, Hayer-Hartl M, Di Liberto M, Hartl FU, Kuriyan J (1997) Crystal structure of the nucleotide exchange factor GrpE bound to the ATPase domain of the molecular chaperone DnaK. Science 276:431–435.
16. Sondermann H, Scheufler C, Schneider C, Hohfeld J, Hartl FU, Moarefi I (2001) Structure of a Bag/Hsc70 complex: convergent functional evolution of Hsp70 nucleotide exchange factors. Science 291:1553–1557.
17. Xu Z, Page RC, Gomes MM, Kohli E, Nix JC, Herr AB, Patterson C, Misra S (2008) Structural basis of nucleotide exchange and client binding by the Hsp70 cochaperone Bag2. Nat Struct Mol Biol 15:1309–1317.
18. Arakawa A, Handa N, Ohsawa N, Shida M, Kigawa T, Hayashi F, Shirouzu M, Yokoyama S (2010) The C-terminal BAG domain of BAG5 induces conformational changes of the Hsp70 nucleotide-binding domain for ADP–ATP exchange. Structure 18:309–319.
19. Schuermann JP, Jiang J, Cuellar J, Llorca O, Wang L, Gimenez LE, Jin S, Taylor AB, Demeler B, Morano KA, Hart PJ, Valpuesta JM, Lafer EM, Sousa R (2008) Structure of the Hsp110:Hsc70 nucleotide exchange machine. Mol Cell 31:232–243.
20. Polier S, Dragovic Z, Hartl FU, Bracher A (2008) Structural basis for the cooperation of Hsp70 and Hsp110 chaperones in protein folding. Cell 133: 1068–1079.
21. Shomura Y, Dragovic Z, Chang HC, Tzvetkov N, Young JC, Brodsky JL, Guerriero V, Hartl FU, Bracher A (2005) Regulation of Hsp70 function by HspBP1: structural analysis reveals an alternate mechanism for Hsp70 nucleotide exchange. Mol Cell 17:367–379.
22. Brehmer D, Rudiger S, Gassler CS, Klostermeier D, Packschies L, Reinstein J, Mayer MP, Bukau B (2001) Tuning of chaperone activity of Hsp70 proteins by modulation of nucleotide exchange. Nat Struct Biol 8: 427–432.
23. Ha JH, McKay DB (1994) ATPase kinetics of recombinant bovine 70 kDa heat shock cognate protein and its amino-terminal ATPase domain. Biochemistry 33: 14625–14635.
24. Russell R, Jordan R, McMacken R (1998) Kinetic characterization of the ATPase cycle of the DnaK molecular chaperone. Biochemistry 37:596–607.
25. Slepenkov SV, Witt SN (1998) Kinetics of the reactions of the *Escherichia coli* molecular chaperone DnaK with ATP: evidence that a three-step reaction precedes ATP hydrolysis. Biochemistry 37:1015–1024.
26. Gassler CS, Wiederkehr T, Brehmer D, Bukau B, Mayer MP (2001) Bag-1M accelerates nucleotide release for human Hsc70 and Hsp70 and can act concentration-dependent as positive and negative cofactor. J Biol Chem 276:32538–32544.
27. Vagin AT (1997) A. MOLREP: an automated program for molecular replacement. J Appl Crystallogr 30: 1022–1025.
28. O'Brien MC, McKay DB (1995) How potassium affects the activity of the molecular chaperone Hsc70. I. Potassium is required for optimal ATPase activity. J Biol Chem 270:2247–2250.
29. Palleros DR, Reid KL, Shi L, Welch WJ, Fink AL (1993) ATP-induced protein-Hsp70 complex dissociation requires K+ but not ATP hydrolysis. Nature 365:664–666.
30. Flaherty KM, Wilbanks SM, DeLuca-Flaherty C, McKay DB (1994) Structural basis of the 70-kilodalton heat shock cognate protein ATP hydrolytic activity. II. Structure of the active site with ADP or ATP bound to wild type and mutant ATPase fragment. J Biol Chem 269:12899–12907.
31. O'Brien MC, Flaherty KM, McKay DB (1996) Lysine 71 of the chaperone protein Hsc70 Is essential for ATP hydrolysis. J Biol Chem 271:15874–15878.
32. Wilbanks SM, McKay DB (1998) Structural replacement of active site monovalent cations by the epsilon-amino group of lysine in the ATPase fragment of bovine Hsc70. Biochemistry 37:7456–7462.
33. O'Brien MC, McKay DB (1993) Threonine 204 of the chaperone protein Hsc70 influences the structure of the active site, but is not essential for ATP hydrolysis. J Biol Chem 268:24323–24329.
34. Shida M, Arakawa A, Ishii R, Kishishita S, Takagi T, Kukimoto-Niino M, Sugano S, Tanaka A, Shirouzu M, Yokoyama S (2010) Direct inter-subdomain interactions switch between the closed and open forms of the Hsp70 nucleotide-binding domain in the nucleotide-free state. Acta Crystallogr D Biol Crystallogr 66: 223–232.
35. Otwinowski Z, Minor W (1997) Processing of X-ray diffraction data collected in oscillation mode. Methods Enzymol 276:307–326.
36. Brünger AT, Adams PD, Clore GM, DeLano WL, Gros P, Grosse-Kunstleve RW, Jiang J-S, Kuszewski J,

Nilges M, Pannu NS, Read RJ, Rice LM, Simonson T, Warren GL (1998) Crystallography & NMR system: a new software suite for macromolecular structure determination. Acta Crystallogr D Biol Crystallogr 54: 905–921.
37. Vagin AA, Steiner RA, Lebedev AA, Potterton L, McNicholas S, Long F, Murshudov GN (2004) REFMAC5 dictionary: organization of prior chemical knowledge and guidelines for its use. Acta Crystallogr D Biol Crystallogr 60:2184–2195.
38. Emsley P, Lohkamp B, Scott WG, Cowtan K (2010) Features and development of Coot. Acta Crystallogr D Biol Crystallogr 66:486–501.
39. Harding MM (2006) Small revisions to predicted distances around metal sites in proteins. Acta Crystallogr D Biol Crystallogr 62:678–682.
40. Laskowski RA, MacArthur MW, Moss DS, Thornton JM (1993) PROCHECK: a program to check the stereochemical quality of protein structures. J Appl Crystallogr 26:283–291.